Food Chemistry 434 (2024) 137329

Contents lists available at ScienceDirect

Food Chemistry

journal homepage: www.elsevier.com/locate/foodchem

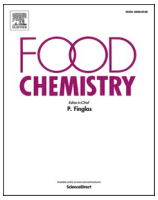

The influence of thermodynamic qualities of a solvent on the physicochemical properties of lentil protein concentrate – Second virial coefficient study

Daniel Żmudziński [a], Urszula Goik [a], Paweł Ptaszek [b,*], Anna Ptaszek [a], Jakub Barbasz [c], Joanna Banaś [d], Dawid Lupa [e]

[a] Agriculture University in Krakow, Faculty of Food Technology, Department of Engineering and Machinery in Food Industry, Balicka 122, 30-149 Kraków, Poland
[b] Agriculture University in Krakow, Faculty of Food Technology, Department of Fermentation Technology and Microbiology, Balicka 122, 30-149 Kraków, Poland
[c] Jerzy Haber Institute of Catalysis and Surface Chemistry Polish Academy of Sciences, Niezapominajek 8, 30-239 Kraków, Poland
[d] Agriculture University in Krakow, Faculty of Food Technology, Department of Biotechnology and General Technology of Food, Balicka 122, 30-149 Kraków, Poland
[e] Jagiellonian University, Faculty of Physics, Astronomy, and Applied Computer Science, M. Smoluchowski Institute of Physics, Łojasiewicza 11, 30-348 Kraków, Poland

ARTICLE INFO

Keywords:
Lentil protein
Surface tension
Second virial coefficient
Hydrodynamic properties
Theta conditions

ABSTRACT

A protein concentrate (75.2%) was obtained from some *Lens culinaris* L. seeds. The osmotic, hydrodynamic and surface properties of protein concentrate aqueous solutions were studied with the help of membrane osmometry, dynamic light scattering, ζ-potential and the pendant drop method, in a wide range of protein concentrate concentrations and *pH* conditions. The second virial coefficient was determined in the range of *pH* 2–9. Two theta points ($pH \sim 5$ and $pH \sim 8$) were found. The change of the hydrodynamic radii as a function of pH and scattering vector was analysed. It was found that the change of the solvent parameters (*pH*) has a significant influence on the surface tension value. This phenomenon was related to the values of the second virial coefficient and the translational diffusion coefficient. The increase in the value of the diffusion coefficient (smaller hydrodynamic radius) resulted in faster interface formation at the gas–liquid interface.

1. Introduction

Legumes (lentils, beans, peas, chickpeas) are one of the most popular human food sources. Unlike animal protein, the production of which is a significant environmental burden, legume seeds can be and are widely used as the main source of protein in a diet. They are the staple food for over a billion people. Thanks to their chemical composition, they are a source of starch, fibre and proteins, which with further processing can be used to produce various new products. Lentils (*Lens culinaris Medik* L.) belonging to the *Fabaceae* L. family is a popular plant grown mainly in Canada, the USA, India, Australia and the Middle East. It is in high demand worldwide and shows the highest growth rates in production and consumption compared to other legumes (Khazaei et al., 2019). Like most legumes, it is rich in proteins and may contain from 20.6% to 31.4% of them (Urbano, Porres, Frias, & Vidal-Valverde, 2007), however, its amount depends on the genetic variety and place of cultivation and may, in extreme cases, amount to 10.5 up to 36.4% (Khazaei et al., 2019). About 50% of proteins are globulins containing legumin and vicilin-like proteins with molecular weights of approximately 60*kDa* and in the range of 50 −80*kDa*, respectively (Barbana & Boye, 2011). In addition, lentil is a plant that is rich in fibre and only contains a small amount of fat. Its seeds also have high antioxidant activity compared to other legume species, mainly due to specific phenolic compounds (Grela et al., 2017). Lentil proteins are characterised by a high digestibility of 83% and have great application possibilities in the production of food products (Barbana & Boye, 2013; El-Sohaimy, Sitohy, & El-Masry, 2007; Boye et al., 2010). All this means that detailed knowledge and the understanding of the physicochemical properties of a plant proteins ensures a better connection with the functional properties and, at the same time, with better applicability of the tested compounds. This will enable the development of new functional food products.

So far, the physicochemical or functional properties of the lentil proteins and/or their formulations have been tested in a relatively small *pH* range. Most commonly, it ranged from neutral to alkaline or from acid to neutral. The test preparations were obtained by protein extraction under various conditions of *pH* and temperature (Chang, Tu, Ghosh,

* Corresponding author.
E-mail address: pawel.ptaszek@urk.edu.pl (P. Ptaszek).

https://doi.org/10.1016/j.foodchem.2023.137329
Received 9 August 2022; Received in revised form 7 June 2023; Accepted 28 August 2023
Available online 8 September 2023

& Nickerson, 2015; Joshi et al., 2012; Asli Can, Nicholas, & Michael, 2011; Bora, 2002). In the available literature, it can be seen that a series of tests of their physicochemical and functional properties have been performer like: solubility, surface tension or interfacial tension, protein structure, ζ-potential, surface hydrophobicity and molecular mass distribution (Alonso-Miravalles et al., 2019; Tabilo-Munizaga et al., 2019; Jarpa-Parra et al., 2014; Jarpa-Parra et al., 2015). Also functional properties of protein isolates or concentrates were analysed (Alonso-Miravalles et al., 2019; Jarpa-Parra et al., 2014; Jarpa-Parra et al., 2015; Tabilo-Munizaga et al., 2019).

In the above works, the molecular characteristics of proteins using electrophoresis were presented in detail, which allowed for the identification of individual fractions of storage proteins present in lentil seeds. The changes in ζ-potential and the solubility as a function of *pH* were studied (Alonso-Miravalles et al., 2019), and the isoelectric point has been determined (Jarpa-Parra et al., 2015). On the other hand, the measurements of the hydrodynamic radius for the proteins molecules and their aggregates and the external surface value are described in a narrower *pH* range (Jarpa-Parra et al., 2014; Jarpa-Parra et al., 2015). A review of the literature on these proteins revealed some shortcomings related to their characteristics over a wide *pH* range. There are no results or discussions in the literature regarding the deeper view into the interactions between proteins and solvent with the help of DLS in the wide range of scattered angle or membrane osmometry and the second virial coefficient (A_2). This coefficient is a measure of the thermodynamic quality of the solvent and its effect on the behaviour of the protein in the solution (Boire et al., 2019). The A_2 analysis makes it possible to predict the stability of protein solutions and their preparations in solutions Velev, Kaler, and Lenhoff (1998), Tessier et al. (2004). The aim of this study was to obtain a lentil protein concentrate using the precipitation method at the isoelectric point and performing a comprehensive analysis of the physicochemical properties of lentil protein concentrate solutions using techniques such as membrane osmometry, measurements of specific viscosity and translational diffusion coefficient (DLS). The hanging drop technique was used to measure the surface tension. The paper also focuses on the discussion of the obtained results in the protein-solvent and protein–protein interactions, with the use of the interpretation based on the second virial coefficient (A_2).

2. Materials and methods

2.1. Materials

The material used for the research were edible lentils from a local market. The dry seeds were ground and then homogenised in water at a ratio of 1:9 under conditions 16 kRPM. The homogenate was alcalified (alcalized) to $pH = 10.5$, (1 M NaOH) constantly stirring (2 kRPM) for 1hour at a temperature of 20°C.The mixture was then centrifuged at 3000*g* for 10 min. The obtained supernatant was acidified to $pH = 4.0$ (1 M HCl) to reach the isoelectric point and centrifuged under the same conditions. The sediment (of the protein) after precipitation at the isoelectric point was washed with water and centrifuged again (Jarpa-Parra et al., 2014). The purified sediment was then transferred to water and the *pH* of the system was normalised to 6.8. The obtained normalised protein sediment was frozen and then lyophilised. A conversion factor of 6.25 (ISO 1871:2009, 2009) was used to convert nitrogen values to protein content. The protein content of lyophilised lentil protein extract was (75.2 ± 0.6) $g/100g$, indicating that other components like carbohydrates $(12.6 \pm 0.1\ g/100g)$ or minerals $(5.5 \pm 0.1\ g/100g)$ could be precipitated with proteins. The nitrogen solubility was determined by the method of Beuchat et al. (1975) at different pH levels. The dispersions were shaken for an hour at 20°C and then centrifuged at 5 kRPM for 10 min. The nitrogen content of the supernatant was determined using the Kjeldahl method. Nitrogen solubility *S* was expressed as a percentage of the nitrogen in the solution to that of the total nitrogen in the sample. According to solubility results, all PC concentrations are expressed as related to soluble protein content. In the preparation of the solutions, the solubility of the protein concentrate at a different *pH* was taken into account, insoluble residues were removed and the concentration of the solution was checked.

2.2. Material characterisation

2.2.1. Electrophoretic research

Electrophoresis was performed on a polyacrylamide gel by SDS–PAGE in a reducing medium produced by 2-mercaptoethanol (Laemmli, 1970). A Vertical Mini-Vertigel 2 electrophoresis apparatus (Apelex, Lisses, France), cooperating with the PS 608 power supply (Apelex, Lisses, France), was used. A portion of the lyophilised protein was dissolved in deionised water, and then mixed in Eppendorf tubes with the reducing solution (0.125*M* TrisCl, 4% SDS, 20% glycerol, 2% 2-mercaptoethanol, *pH* 6.8). The sample was placed in a water bath for 90 s, and after cooling, was injected onto a previously prepared bilayer polyacrylamide gel. The thickening layer had a concentration of 4% and the separating layer was 12.5%. The denaturation procedure was also used for the standard proteins. DC separations at 25 *mA* were performed for 90 *min* at a voltage of 100 to 260 *V*. The SDS6H2 and SDS7 protein kits (Sigma–Aldrich, St. Louis, USA) were used as standards. The gels after staining in Coomassie Blue R-250 solution and then being scanned. Gel scans were analysed using the GelAnalyser 2010a software (Lazar, 2022).

2.2.2. Hydrophobicity of isolate proteins concentrate

The surface hydrophobicity (*H*) was determined by the fluorimetric method (Hayakawa & Nakai, 1985) with 1-anilino-8-naphthalene sulfonate (ANS) as the fluorescent indicator. Several solutions of the given hydrolyzate were prepared with a protein concentration of 0.025 to 0.5 $g{\cdot}L^{-1}$ and the ANS solution (8.0 $mmol{\cdot}L^{-1}$) was added to them. Fluorescence intensity (FI) was measured on a Cary-Eclipse spectrofluorimeter (Varian, Palo Alto, CA, USA) at 390 and 470 *nm* for excitation and emission, respectively. The tests were carried out on 1% PC solutions (converted to protein) a $pH(2-9), \Delta pH = 1$.

2.3. The effect of the concentration and pH on selected properties of concentrate solutions

2.3.1. Density and viscosity measurements

The density of the buffer solutions and protein concentrate solutions were measured at 25 °C. The density meter DMA 5001 (Anton Paar, Graz, Austria) was used for the measurements. The tests were carried out for the following concentration range at each analysed $pH(2-9), \Delta pH = 1$: $(c = 10^{-3}, 10^{-2}, 10^{-1}, 2{\cdot}10^{-1}, 3{\cdot}10^{-1}, 4{\cdot}10^{-1}, 5{\cdot}10^{-1}, 6{\cdot}10^{-1}, 7{\cdot}10^{-1})$ $g{\cdot}mL^{-1}$.

Viscosity measurements were made with an Ubbelohde viscometer at 25 °C, the time of flow through the capillary was measured with ViscoClock (SI ANALYTICS, Weilheim, Germany) with an accuracy of 0.01 *s*. The range of the analysed concentrations of protein preparations and *pH* was the same as for the density measurements.

The viscosity η of the solutions was calculated using the following equation:

$$\eta = \eta_{solv} \cdot \frac{\rho \cdot t}{\rho_0 \cdot t_0} \tag{1}$$

where: η_{solv} and ρ, ρ_0, t i t_0 are respectively: viscosity of solvent, density and time of flow through the capillary for solutions and water (Masuelli, 2014). As the first step (Macosko, 1994), the specific viscosity η_{sp} and the reduced viscosity, η_{red}, independent of the protein concentration *c* were calculated:

$$\eta_{red} = \frac{\frac{\eta}{\eta_0} - 1}{c} = \frac{\eta_{sp}}{c} \tag{2}$$

For all the tested samples the measurements were repeated three times.

2.3.2. Membrane osmometry

Osmometric measurements were made using an Osmomat 090 membrane osmometer (Gonotec, Berlin, Germany). The tests were carried out for the *pH* (2–9) at 25°C for the concentration range of the protein concentrate from $5{\cdot}10^{-4}$ to $7{\cdot}10^{-3}$ $g{\cdot}mL^{-1}$. All measurements were carried out with a 10 $kg{\cdot}mol^{-1}$ cut-off membrane. For all tested samples the measurements were done and repeated four times.

The obtained results were subject to analysis involving the estimation of parameters of the osmotic equation of state:

$$\frac{\pi}{c} = RT\cdot\left[\frac{1}{M_n} + A_2\left(T\right)\cdot c + \ldots\right] \tag{3}$$

where: c - the concentration of the dissolved PC, M_n - the number average osmotic molecular mass, $A_2(T)$ - the osmotic virial coefficient, R - the gas constant, T - the absolute temperature. Value of A_2 was estimated by the least square method.

2.3.3. Surface tension

All surface tension measurements were made using the pendant drop method, with a home built device. This device consisted of: a 1/1.2" CMOS sensor, with a resolution 1920x1200 pixels (Grasshopper 3, Point Grey Richmond, Canada), a 300× magnification lens, an LED light source and a syringe with a stepper motor and a screw. The syringe was tipped with a 0.62 *mm* diameter needle. Arduino UNO was used to control the syringe stepper motor. The image acquisition software was written in Python 3. Then the received images were analysed using the OpenDrop (Huang et al., 2021) program. For each tested solution, 1000 images were taken within 1000 s. The measurements were performed for the protein concentrate solutions in the concentration range from 10^{-6} to 10^{-1} $g{\cdot}mL^{-1}$ ($\Delta c = 10$ $g{\cdot}mL^{-1}$) in $pH(2-9)$.

2.4. The effect of pH on the hydrodynamic properties

2.4.1. ζ - potential

The electrophoretic mobility (μ_e) of proteins (1% solution - 0.01 $g{\cdot}mL^{-1}$) was determined by Zetasizer Nano ZS Malvern (Malvern, Malvern, UK) device. The results were obtained in aqueous solutions at pH (2–9), $\Delta pH = 1$. A Britton–Robinson buffer was used in each case. The ζ-potential (ζ) of protein concentrate was calculated based on the Smoluchowski-Henry equation:

$$\zeta = \frac{3\eta}{2\varepsilon F(\kappa a)}\mu_e \tag{4}$$

where: the $F(\kappa a)$ is a dimensionless function of the parameter κa, the symbol a corresponds to the radius of the particle (ie. hydrodynamic radius R_h), ε is a dielectric constant, η is the viscosity of solvent, μ_e is an electrophoretic mobility and κ is the Debye length.

2.4.2. Dynamic light scattering (DLS)

The dynamic light scattering measurement was performed on $0.01g{\cdot}mL^{-1}$ solutions of broad lentil protein concentrate (calculated for protein) made in a Britton-Robinson buffer with *pH* 2–9 with step 1. The solutions were filtered using a 5 *μm* syringe filter, to ensure that undissolved material would not be in the path of the laser beam. Filters with smaller cut-off effect were not used due to the possible elimination of aggregates. A set consisting of an Brookhaven Instruments (Holtsville, NY, USA) goniometer, equipped with a laser that used a wavelength of 532 *nm* and a power of 50 *mW* was used to characterise the hydrodynamic properties of PC solutions. The determination of the autocorrelation function took place in the range of measurement angles from 30° to 150°, at the temperature of 25°C. For all tested samples the measurements were done in five repetitions. This allowed to determine the scattering vector (q) in the analysed range of angles:

$$q = \frac{4\pi n}{\lambda}\sin\left(\frac{\theta}{2}\right) \tag{5}$$

where: n - refractive index of solution; λ - lenght of light wave; θ - scattering angle, and the translational diffusion coefficient:

$$\overline{D} = \frac{\overline{\Gamma}}{q^2} \tag{6}$$

where: $\overline{D}$ - translational diffusion coefficient; $\overline{\Gamma}$ - average decay, calculated using method of cumulants form autocorrelation function (Koppel (1972)).

The hydrodynamic radius was calculated as follow:

$$R_h = \frac{k_b\cdot T}{6\cdot\pi\cdot\eta\cdot\overline{D}} \tag{7}$$

where: k_b - the Boltzman constant, T - the absolute temperature, η - the viscosity of the solvent at temperature T.

2.5. Statistical analysis

Nonlinear least square method was used for model parameters estimates. Also 5% confidence intervals for a polynomial fittings were calculated. Calculations were carried out using package R (R Core Team (2022)) and Python 3 programing language.

3. Results

3.1. Electrophoresis

Based on the results obtained with SDS–PAGE (Fig. 1) 27 bands were found which can be divided into 4 main groups. These groups were in the following molecular weight ranges: 16–18 *kDa*, 20–28 *kDa* 34–42 *kDa* and 45–66 *kDa*. The lowest molecular weight fractions were probably the γ-vicilin group contaminated with the basic 11S subunit fraction. Two legumins-like 11S fractions have also been identified: the first

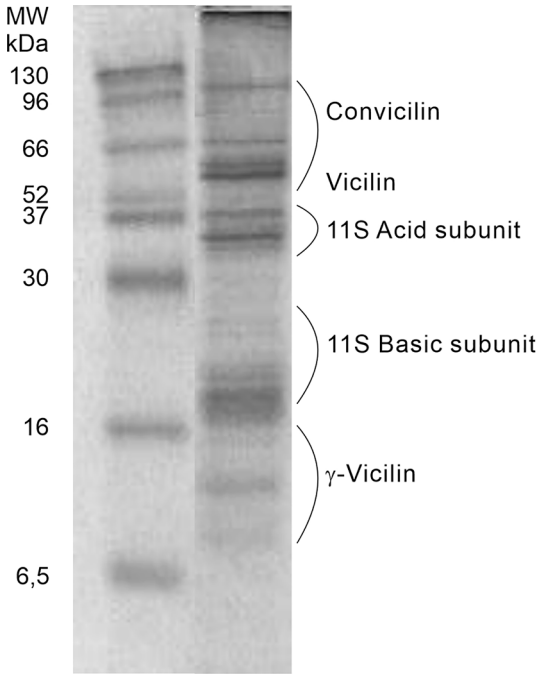

Fig. 1. SDS–PAGE profiles of Lens culinaris L. protein under reduction conditions. Lane: A - protein markers; B - Lens culinaris L. protein concentrate.

one with M_n in the range: 20–28 *kDa*, which were the basic fraction, and the second one with molecular weights (M_n) in the range of 34–42 *kDa*, which were the acid fraction. Proteins with molecular weights from 45 *kDa* and above belonged to the 7S sub-unit and were classified as a vicilin fraction or enriched in the vicilin fraction due to their contamination with this fraction (Derbyshire, Wright, & Boulter, 1976; Lee, Lu, Zhang, Fu, & Huang, 2021).

3.2. The effect of the concentration and pH on selected properties of concentrate solutions

Fig. 2 shows a summary of the physicochemical properties of the solutions protein concentrate (PC) as a function of *pH*. The aim of presenting the results in such a way was to show the influence of *pH* on the shaping of the phenomena occurring in the analysed layouts. The parameters in Fig. 2 have been grouped so that each pair represents related properties of the analysed PC solutions, and together they provide a complete picture of their changes as a function of *pH*.

The relation between the second virial coefficient (A_2) and the hydrophobicity (H_o) of the protein concentrate (PC) as a function of *pH* is shown in Fig. 2. The values of A_2 were estimated according to nonlinear virial Eq. 3 fitted to the measurements result presented in supplementary data (Figure S.1.). The second virial coefficient represents the polymer–solvent and polymer–polymer interactions, which could be shaped among others by the hydrophobicity (H_o) of PC. It can be seen that in the acidic conditions ($pH < 5$) the values of the second virial coefficient

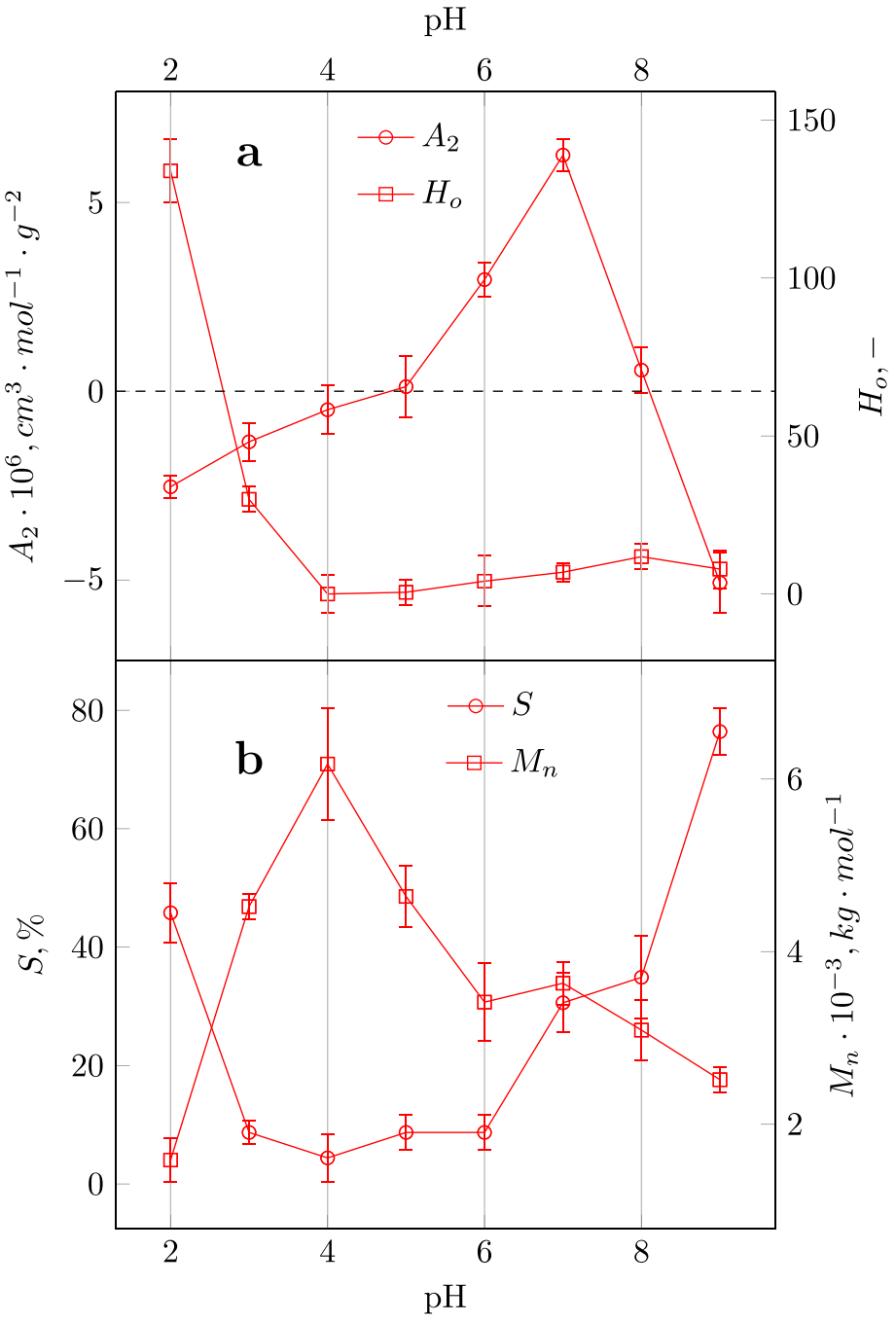

Fig. 2. Properties of PC solutions in function of pH: top - second virial coefficient (A_2) and hydrophobicity (H_o); bottom - solubility (S) and number average osmotic molecular mass M_n (*replications* $n = 5$).

were negative: the acidic residue present in the protein molecules were neutralised (Kiersten et al., 2018), and the affinity of the polymer to the solvent was not high. The H_o in the *pH* range of 2 to 5 is high and decreases with the *pH* growth. For $pH \sim 5$, the value of the second virial coefficient was zero. The zero value of A_2 corresponded to thermodynamic Θ conditions, in which no interaction between the polymer and the solvent is observed (Boire et al., 2019). Close to this *pH* value the H_o reaches minimum. Changing the *pH* to a higher one resulted in an increase in the A_2 value and slight rise of *pH* values. At $pH = 7$, the second virial coefficient reached its maximum, reflecting the good affinity of the protein concentrate for the solvent. Above neutral *pH*, the A_2 value decreased again and changed its sign at $pH \sim 8$. This behaviour indicates that the Θ conditions have been reached again. This behaviour is typical of plyampholyte systems, i.e. systems containing zwitterions (Kiersten et al., 2018).

Belonging to another group of closely related physical quantities is hydrophobicity (H_o), the *pH* dependence of which is shown in Fig. 2. The hydrophobicity in an acidic environment has the highest values, which can be explained by a good exposure of hydrophobic groups present in the chains of tested proteins. In these conditions, the ζ-potential values were positive (supplementary data Figure S.2.). At $pH > 3$, a change in the sign of ζ-potential The very low value of H_o indicated the presence of an isoelectric point. Further *pH* change resulted in a slight increase in hydrophobicity. This phenomena resulted from the change in the nature of the medium in which the PC was dissolved. Alkaline residues present in PC proteins were ionised under alcaline conditions, which resulted in partial exposure of hydrophobic groups in these molecules (Kiersten et al., 2018).

The relation between solubility (S) and number average osmotic molecular mass (M_n) was presented in Fig. 2 (bottom). The pH

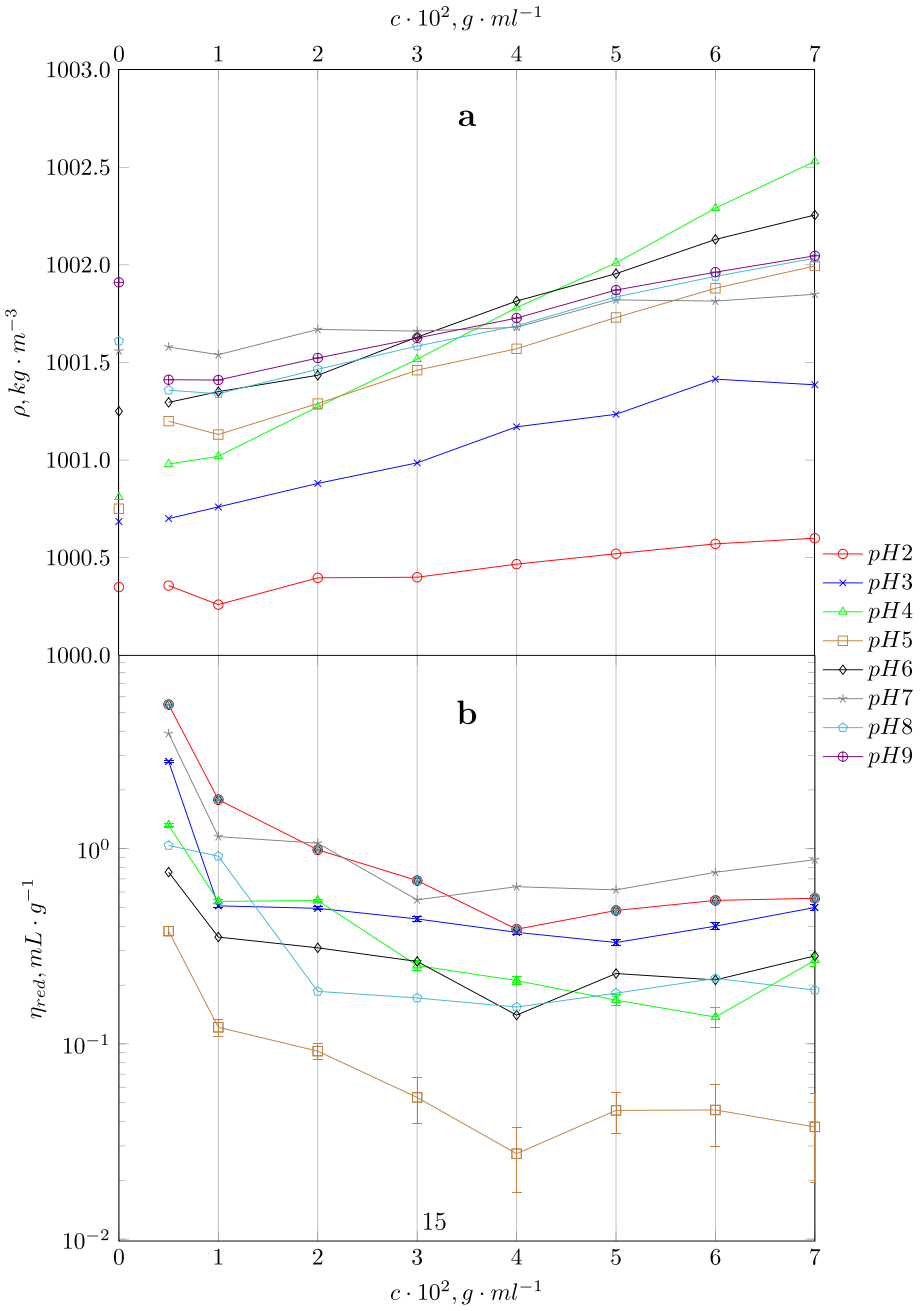

Fig. 3. a - Density; b - reduced viscosity of *Lens culinaris* L. protein concentrate (PC) solutions as a function of concentration for different *pH* values (*replications n = 5*).

dependence of the solubility showed visible minimum characteristic for proteins in the isoelectric point. In this *pH* condition number average molecular mass M_n reaches maximum value of $\sim 6{\cdot}10^3 kg{\cdot}mol^{-1}$. Next M_n values decrease with rising *pH* while the solubility rises to the maximum value at $pH = 9$.

3.2.1. Density and viscosity of PC solutions

Fig. 3a shows the dependence of the density (ρ) on the concentration of the proteins solution for each *pH*. At $pH < 5$, a increase of density with the PC concentration was observed. At $pH = 4$, at an isoelectric point of PC, the slope of the line chart $\rho(c)$ was the greatest. In case of $pH = 5$ and $pH = 6$ the changes in density as a function of PC concentration were not so abrupt. At $pH = 7$ the $\rho(c)$ dependence was characterised by a slight slope of the line chart in relation to the solutions with a different *pH*. PC solutions at $pH = 7$ had the best thermodynamic compatibility, that is high affinity of a protein to a solvent.

The dependence of the reduced viscosity on the *pH* and solution concentration was presented in Fig. 3b. Under the conditions of *pH* range from 2 to 7, the dependence of $\eta_{red}(c)$ was decreasing for first four *pH* conditions and next rising. The changes in the reduced viscosity as a function of *pH* showed the characteristic for the polyelectrolytes behaviour (Lopez & Richtering, 2019). There was not observed a partial

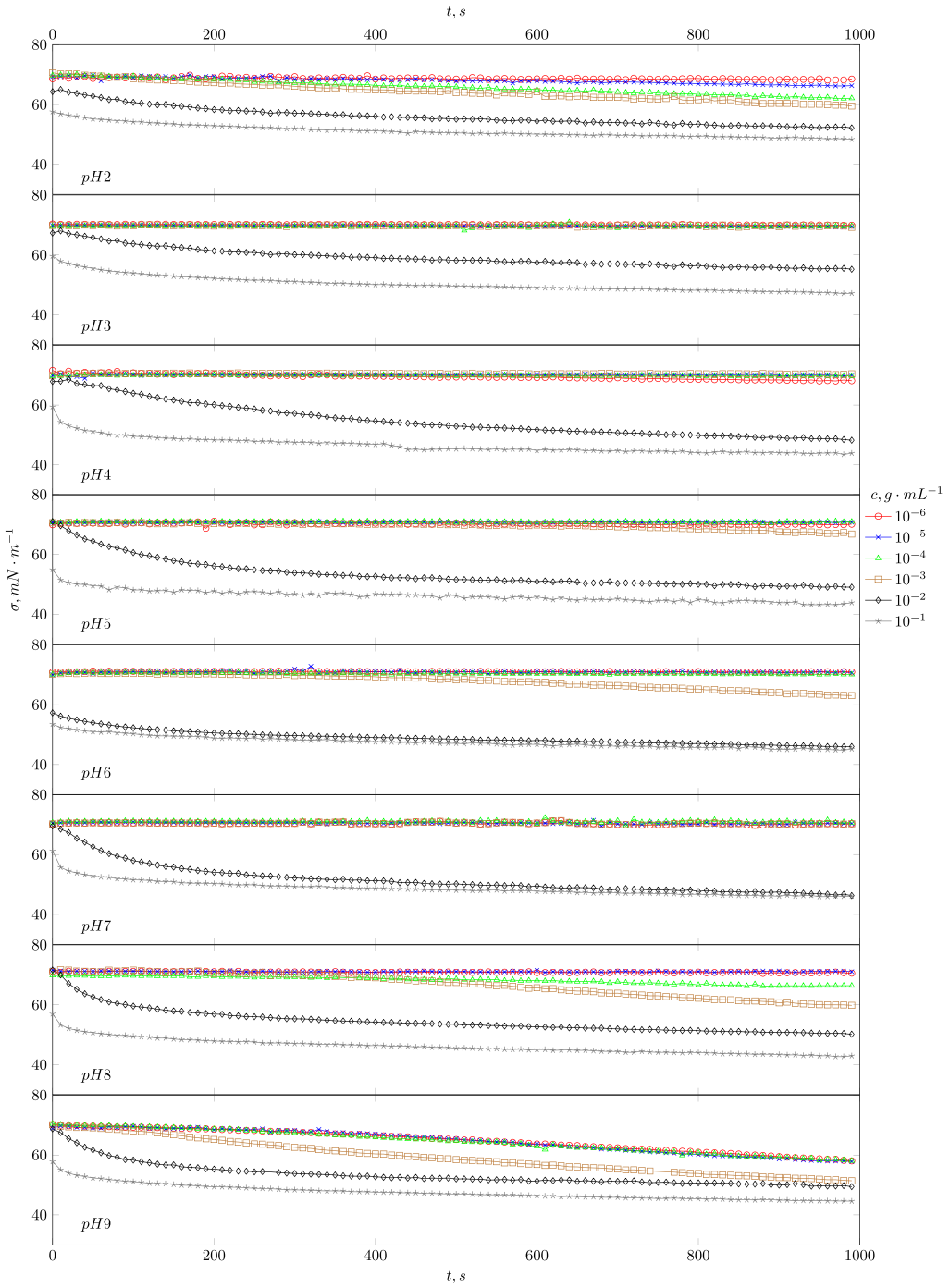

Fig. 4. Surface tension of PC solutions as a function of time for different *pH* and concentrations (*replications* $n = 5$).

hydrolysis in the wide *pH* range during preliminary studies, the presence of aggregates was confirmed by the results from DLS measurements. The increase in *pH* generated a decrease in the value of the reduced viscosity in the entire concentration range. At $pH = 7$ the lowest $\eta_{red}(c)$ values associated with a very high solvent affinity of PC (highest A_2 value) were observed (due to very low values not shown in chart with log scale). For higher values of $pH = 8$ and $pH = 9$, the behaviour of protein molecules in solution was anlogous to the systems with a *pH* lower than 7.

3.2.2. Surface tension of PC solutions

The analysis of the changes in the surface tension of the protein concentrate solution (Fig. 4) showed both the effects of the concentration of PC itself and the dependence on the *pH* value. The dependence of the surface tension on high concentrations (10^{-2} $g{\cdot}ml^{-1}$, 10^{-1} $g{\cdot}ml^{-1}$) resulted in a similar scenario for all *pH* values. In these cases, a rapid decrease in the value of $\sigma(t)$ was observed, followed by a time determination. This phenomenon was due to the presence of a large number of protein molecules in the solution, resulting in rapid layer formation at the gas–liquid interface. At lower concentrations, this effect resulted from interactions in the solution between the PC and solvent. The changes of surface tension as a function of time for PC at $pH = 2$ were visible for the lowest concentration values (10^{-6} $g{\cdot}ml^{-1}$) of the solutions. The phenomenon resulted from the high hydrophobicity generated by the large number of hydrophobic groups present on the protein aggregates external surface and the negative value of A_2 (Fig. 2). Because of the low affinity of PC to the solvent and low number average molecular mass, the protein molecules showed a greater ability to build the interface on a gas–liquid interface. This was reflected in a rapid decrease in surface tension values within the observed time range. The increase in *pH* resulted in a sharp decrease in the number average molecular mass and hydrophobicity (Fig. 2). With the protein-solvent increasing affinity (higher A_2 values) the creation of a gas–liquid interface was limited. At $pH = 5$ and $pH = 6$, small changes in $\sigma(t)$, values were observed in the low PC concentration range. The behaviour of low-concentrated PC solutions at $pH = 7$ showed no change in surface tension. This was due to the very good thermodynamic compatibility of the proteins and the solvent (highest observed A_2 value), therefore the protein molecules did not show any tendency on the gas–liquid interface creation.

At $pH = 8$ and $pH = 9$, the change in surface tension with time was similar to that at $pH = 2$. This was associated with negative A_2 values and the increasing hydrophobicity of the investigated systems (Fig. 2). This meant a greater number of hydrophobic groups present on a external surface and greater affinity of aggregates to the gas–liquid interface creation.

4. Discussion

4.1. The effect of pH on the hydrodynamic properties

The discussion is focused on the properties of PC solution of 0.01 $g{\cdot}ml^{-1}$. In order to better visualise the changes taking place in PC solutions as a function of *pH*, Fig. 5 shows the dependence of the

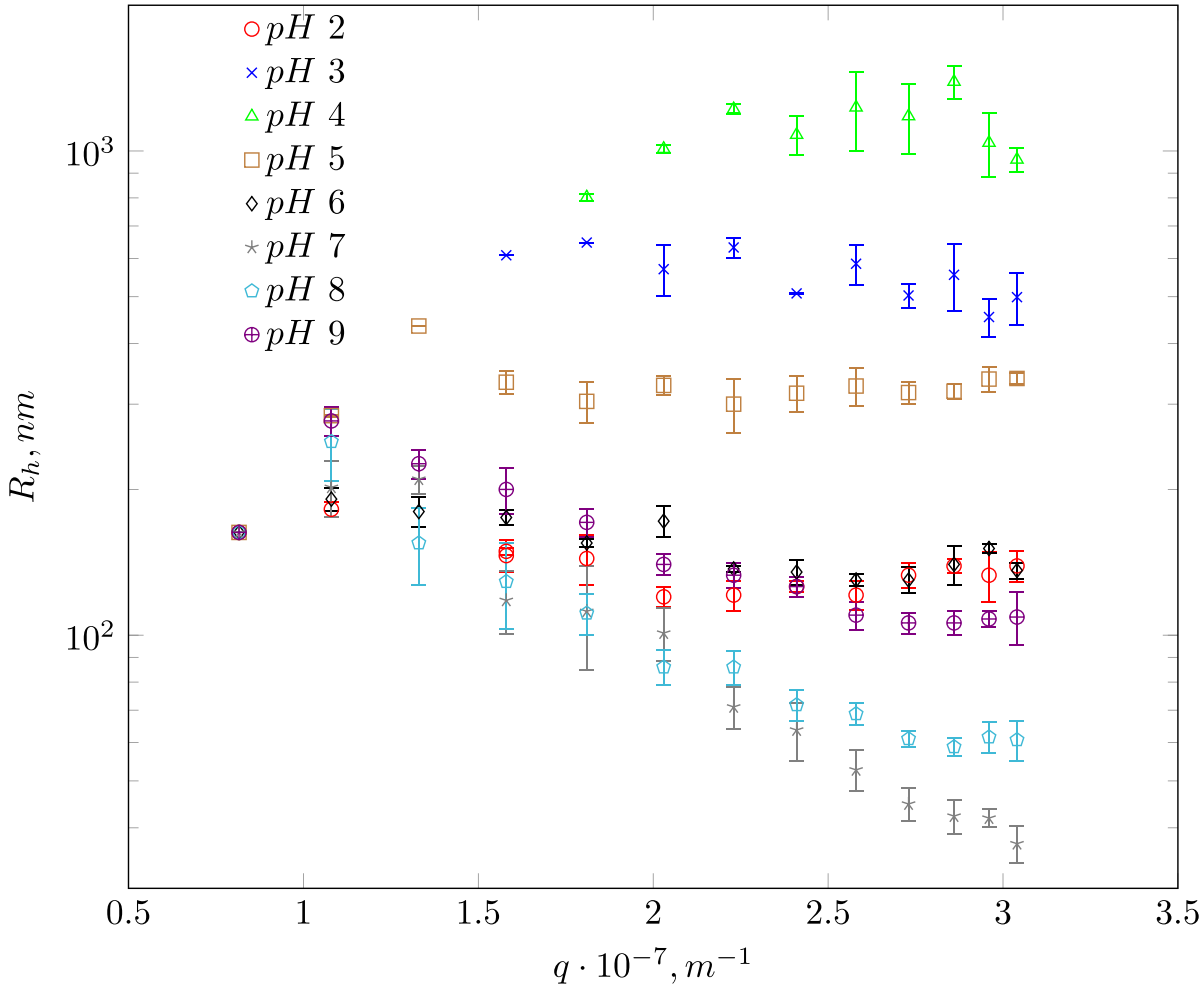

Fig. 5. Hydrodynamic radius (R_h) as a function of the scattering vector (q) at different *pH* conditions for 0.01 $g{\cdot}ml^{-1}$ solution of lentil protein concentrate (*replications* $n = 5$).

hydrodynamic radius of protein chains as a function of the scattering vector (q). Analysis of these relationships showed that the hydrodynamic radius at $pH = 2$ reaches values below 200 nm and remains independent of the scattering vector. This means that, according to the dispersion theory, objects with a similar hydrodynamic radius are present in the solution (Pecora, 1985).Moreover, when compared with the hydrodynamic radius of the single protein molecule the size detected during DLS measurements suggested the presence of aggregates. The protein molecules behaviour was described by a negative A_2 value due to a thermodynamic incompatibility between the biopolymer and solvent. The solvent does not penetrate the molecules (no swelling of the macromolecules was observed), resulting in a low R_h value. Under these conditions, the hydrophobicity (Fig. 2) and ζ-potential (Figure S.2.) are higher due to the ionisation of the acid protein residues and the exposure of the hydrophobic groups. At $pH = 3$, an increase in R_h values in scattering vector function was observed. A similar behaviour was noted in the case of the pH value of 4, where the R_h values were extremely high. The described course of the phenomenon indicates the aggregation of the molecules and results from the isoelectric point conditions. At $pH = 5$, the R_h value decreased significantly and did not change with the increasing scattering vector value. This meant that a protein aggregation took place close to the isoelectric point. This was favoured by an acidic pH value. The protein-solvent, protein–protein interaction, plays a key role in the aggregation phenomena. This effect is indicated by the second viral coefficient (A_2) and the values of the number average molecular mass (Fig. 2). In the protein concentrate systems studied, the second virial coefficient was strongly dependent on the pH of the solution, with the sign changed twice. This means that the Θ conditions have occurred twice. In accordance with the thermodynamics of polymer solutions, this meant a change in the type of interactions between the polymer and the solvent (Kiersten et al., 2018; Ersch, Meijvogel, van der Linden, Martin, & Venema, 2016). From the polymer science point of view, the change of the sign of A_2 means such conditions in which there is no interaction of the solvent with the polymer. Also, the zero value of H_o (Fig. 2) and ζ-potential (Figure S.2.) indicated the lack of solvent-polymer interactions. Under these conditions, the highest R_h value was observed (Fig. 5). These phenomena are commonly used in the separation of plant proteins by (Bonneté & Vivarès, 2002).

When the isoelectric point ($pH \sim 4$) is exceeded, the hydrodynamic radius value decrease rapidly and the mobility of the protein concentrate aggregates in the solution increases (higher diffusion coefficient). As Fig. 5 shows, the R_h values remained constant in the function of the scattering vector. These phenomena have been associated with positive A_2 values reflecting good thermodynamic compatibility between the polymer and the solvent. It also had a significant effect on the decrease of reduced viscosity, what in combination with the slight increase in hydrophobicity (H_o) (Fig. 2) led to a noticeable decrease in surface tension at low concentrations of protein concentrate. At pH values above the isoelectric point, the hydrophobic groups of proteins began to reopen and were present on the surface of the aggregates. The described phenomena contributed to the gas–liquid interface creation and the reduction of the surface tension values. The lowest R_h values were observed for the neutral pH. This was the result of the very good thermodynamic compatibility of PC and the solvent. Under these pH conditions, the protein molecules forming the aggregates showed a higher affinity for the solvent compared to lower pH values. Due to their small size, their mobility improved, which manifested itself in small hydrodynamic radius values. In this case, the second viral coefficient (A_2) has reached the maximum (Fig. 2). This corresponded to the greatest affinity of PC molecules to this solvent. In addition, near zero values for reduced viscosity were observed and no significant decrease in surface tension was observed. The change in pH to 8 resulted in a sharp decrease in A_2 values including the change in sign (+/-). The tested solution again reached the Θ conditions. However, the nature of this phenomenon was different than before ($pH = 4$). Higher H_o-values and completely different R_h-values were observed. In this case, the hydrodynamic radius decreased with increasing scattering vector (q) (Fig. 5). This led to a significant reduction in surface tension in solutions with low concentrations of protein concentrate (Fig. 4).

The behaviour of solutions at $pH = 9$ was described by the highest R_h values and the lowest negative A_2, when compared with $pH = 8$. The maximum value in the solubility of PC and the lowest values of A_2 and ζ-potential were also observed.

5. Conclusions

The presented analysis of the second osmotic virial coefficient estimated for the solutions of the protein concentrate from lentil seeds (*Lens culinaris* L.) showed two pH dependent Θ points. This is a characteristic phenomenon of polyampholyte. The second viral coefficient analysis proved to be a very effective tool for the detailed characterisation of this type of phenomenon. In combination with the analysis of the physicochemical parameters like reduced viscosity or surface tension of PC solutions allows the complete picture of their behaviour over a broad pH range. Knowledge of these properties is crucial for further investigation of the functional properties of the obtained concentrates. They can also provide guidance on the design of processes for lentil protein preparations.

Declaration of Competing Interest

The authors declare that they have no known competing financial interests or personal relationships that could have appeared to influence the work reported in this paper.

Data availability

Data will be made available on request.

Acknowledgments

This research was financed by the Ministry of Science and Higher Education of the Republic of Poland in year 2021.

Appendix A. Supplementary material

Supplementary data associated with this article can be found, in the online version, at https://doi.org/10.1016/j.foodchem.2023.137329.

References

Alonso-Miravalles, L., Jeske, S., Bez, J., Busch, M., Krueger, M., Wriessnegger, C. L., O'Mahony, J. A., Zannini, E., & Arendt, E. K. (2019). Membrane filtration and isoelectric precipitation technological approaches for the preparation of novel, functional and sustainable protein isolate from lentils. *European Food Research and Technology, 245*, 1855–1869. https://doi.org/10.1007/s00217-019-03296-y

Asli Can, K., Nicholas, L., & Michael, N. (2011). Emulsifying properties of chickpea, faba bean, lentil and pea proteins produced by isoelectric precipitation and salt extraction. *Food Research International, 44*, 2742–2750. https://doi.org/10.1016/j.foodres.2011.06.012

Barbana, C., & Boye, J. I. (2011). Angiotensin i-converting enzyme inhibitory properties of lentil protein hydrolysates: Determination of the kinetics of inhibition. *Food Chemistry, 127*, 94–101. https://doi.org/10.1016/j.foodchem.2010.12.093

Barbana, C., & Boye, J. I. (2013). In vitro protein digestibility and physico-chemical properties of flours and protein concentrates from two varieties of lentil (lens culinaris). *Food Function, 4*, 310–321. https://doi.org/10.1039/C2FO30204G

Boire, A., Renard, D., Bouchoux, A., Pezennec, S., Croguennec, T., Lechevalier, V., Le Floch-Fouéré, C., Bouhallab, S., & P., M. (2019). Soft-matter approaches for controlling food protein interactions and assembly. Annu Rev Food Sci Technol., 10, 521–539. doi:10.1146/annurev-food-032818-121907.

Bonneté, F., & Vivarès, D. (2002). Interest of the normalized second virial coefficient and interaction potentials for crystallizing large macromolecules. *Acta Crystallographica Section D, 58*, 1571–1575. https://doi.org/10.1107/S090744490201418X

Bora, P. S. (2002). Functional properties of native and succinylated lentil (lens culinaris) globulins. *Food Chemistry, 77*, 171–176. https://doi.org/10.1016/S0308-8146(01)00332-6

Boye, J., Aksay, S., Roufik, S., Ribéreau, S., Mondor, M., Farnworth, E., & Rajamohamed, S. (2010). Comparison of the functional properties of pea, chickpea

and lentil protein concentrates processed using ultrafiltration and isoelectric precipitation techniques. *Food Research International, 43*, 537–546. https://doi.org/10.1016/j.foodres.2009.07.021

Chang, C., Tu, S., Ghosh, S., & Nickerson, M. (2015). Effect of ph on the inter-relationships between the physicochemical, interfacial and emulsifying properties for pea, soy, lentil and canola protein isolates. *Food Research International, 77*, 360–367. https://doi.org/10.1016/j.foodres.2015.08.012

Derbyshire, E., Wright, D., & Boulter, D. (1976). Legumin and vicilin, storage proteins of legume seeds. *Phytochemistry, 15*, 3–24. https://doi.org/10.1016/S0031-9422(00)89046-9

El-Sohaimy, S., Sitohy, M., & El-Masry, R. (2007). Isolation and partial characterization of chickpea, lupine and lentil seed proteins. *World Journal of Agricultural Sciences, 3*, 123–129.

Ersch, C., Meijvogel, L. L., van der Linden, E., Martin, A., & Venema, P. (2016). Interactions in protein mixtures. part i: Second virial coefficients from osmometry. *Food Hydrocolloids, 52*, 982–990. https://doi.org/10.1016/j.foodhyd.2015.07.020

Grela, E. R., Kiczorowska, B., Samolinska, W., Matras, J., Kiczorowski, P., Rybinski, W., & Hanczakowska, E. (2017). Chemical composition of leguminous seeds: part i—content of basic nutrients, amino acids, phytochemical compounds, and antioxidant activity. *European Food Research and Technology, 243*, 1385–1395. https://doi.org/10.1007/s00217-017-2849-7

Hayakawa, S., & Nakai, S. (1985). Relationships of hydrophobicity and net charge to the solubility of milk and soy proteins. *Journal of Food Science, 50*, 486–491. https://doi.org/10.1111/j.1365-2621.1985.tb13433.x

Huang, E., Skoufis, A., Denning, T., Qi, J., Dagastine, R., Tabor, R., & Berry, J. (2021). OpenDrop: Open-source software for pendant drop tensiometry & contact angle measurements. *Journal of Open Source Software, 6*(58), 2604–2606. https://doi.org/10.21105/joss.02604

ISO 1871:2009 (2009). Food and Feed Products – General Guidelines for the Determination of Nitrogen by the Kjeldahl Method. Standard International Organization for Standardization Geneva, CH.

Jarpa-Parra, M., Bamdad, F., Tian, Z., Zeng, H., Temelli, F., & Chen, L. (2015). Impact of ph on molecular structure and surface properties of lentil legumin-like protein and its application as foam stabilizer. *Colloids and Surfaces B: Biointerfaces, 132*, 45–53. https://doi.org/10.1016/j.colsurfb.2015.04.065

Jarpa-Parra, M., Bamdad, F., Wang, Y., Tian, Z., Temelli, F., Han, J., & Chen, L. (2014). Optimization of lentil protein extraction and the influence of process ph on protein structure and functionality. *LWT - Food Science and Technology, 57*, 461–469. https://doi.org/10.1016/j.lwt.2014.02.035

Joshi, M., Adhikari, B., Aldred, P., Panozzo, J., Kasapis, S., & Barrow, C. (2012). Interfacial and emulsifying properties of lentil protein isolate. *Food Chemistry, 134*, 1343–1353. https://doi.org/10.1016/j.foodchem.2012.03.029

Khazaei, H., Subedi, M., Nickerson, M., Martínez-Villaluenga, C., Frias, J., & Vandenberg, A. (2019). Seed protein of lentils: Current status, progress, and food applications. *Foods, 8*. https://doi.org/10.3390/foods8090391

Kiersten M., R., Stefan, R., Ashutosh, C., & Rohit V., P. (2018). Advances in understanding stimulus-responsive phase behavior of intrinsically disordered protein polymers. Journal of Molecular Biology, 430, 4619–4635. doi:10.1016/j.jmb.2018.06.031.

Koppel, D. E. (1972). Analysis of macromolecular polydispersity in intensity correlation spectroscopy: The method of cumulants. *The Journal of Chemical Physics, 57*, 4814–4820. https://doi.org/10.1063/1.1678153

Laemmli, U. K. (1970). Cleavage of structural proteins during the assembly of the head of bacteriophage t4. *Nature, 227*, 680–685. https://doi.org/10.1038/227680a0

Lazar, I. (2022). GelAnalyzer 19.1. URL: www.gelanalyzer.com.

Lee, H. W., Lu, Y., Zhang, Y., Fu, C., & Huang, D. (2021). Physicochemical and functional properties of red lentil protein isolates from three origins at different ph. *Food Chemistry, 358*, 129749. https://doi.org/10.1016/j.foodchem.2021.129749

Lopez, C. G., & Richtering, W. (2019). Viscosity of semidilute and concentrated nonentangled flexible polyelectrolytes in salt-free solution. *The Journal of Physical Chemistry B, 123*, 5626–5634. https://doi.org/10.1021/acs.jpcb.9b03044

Macosko, C. (1994). Rheology: Principles, Measurements, and Applications. *Wiley - VCH*.

Masuelli, M. (2014). Mark-houwink parameters for aqueous-soluble polymers and biopolymers at various temperatures. *Journal of Polymer and Biopolymer Physics Chemistry, 2*, 37–43. https://doi.org/10.12691/jpbpc-2-2-2

Pecora, R. (1985). Dynamic Light Scattering. *Applications of Photon Correlation Spectroscopy*. Plenum Press.

R Core Team. (2022). *R: A Language and Environment for Statistical Computing*. Austria: R Foundation for Statistical Computing Vienna. URL: http://www.R-project.org/.

Tabilo-Munizaga, G., Villalobos-Carvajal, R., Herrera-Lavados, C., Moreno-Osorio, L., Jarpa-Parra, M., & Perez-Won, M. (2019). Physicochemical properties of high-pressure treated lentil protein-based nanoemulsions. *LWT, 101*, 590–598. https://doi.org/10.1016/j.lwt.2018.11.070

Tessier, P. M., Sandler, S. I., & Lenhoff, A. M. (2004). Direct measurement of protein osmotic second virial cross coefficients by cross-interaction chromatography. *Protein Science, 13*, 1379–1390. https://doi.org/10.1110/ps.03419204

Urbano, G., Porres, J. M., Frias, J., & Vidal-Valverde, C. (2007). *Nutritional value* ((1st ed.).). https://doi.org/10.1007/978-1-4020-6313-8

Velev, O., Kaler, E., & Lenhoff, A. (1998). Protein interactions in solution characterized by light and neutron scattering: Comparison of lysozyme and chymotrypsinogen. *Biophysical Journal, 75*, 2682–2697. https://doi.org/10.1016/S0006-3495(98)77713-6